ELECTRON BEAM DYNAMICS SIMULATION FOR ELECTRON LENSES*

S. Sadovich[†], A. Rossi, CERN, Geneva, Switzerland
G. Stancari, FNAL, Batavia, USA

Abstract

A test stand is under construction at CERN to study high perveance electron guns, electron beam dynamics, and electron beam diagnostics for electron lenses. It will be used to test electron guns for the Hollow Electron Lenses under consideration for beam halo control for High Luminosity LHC (CERN), and for the Space Charge Compensation at SIS18 (GSI) in the frame of the EU funded ARIES project.

In order to prepare for this test stand, simulations will be presented and compared with experiments undertaken at the Fermilab (FNAL) electron lens test stand. These were conducted using a hollow electron gun, with the magnetic field configuration and beam current varied to study their effect. The impact of imperfections on the beam dynamics and overall quality of the electron beam will be discussed. A method for comparing experimental data with simulation is also presented to allow bench-marking of the computer models and simulation tools that will later be applied to the analysis of measurements performed at CERN.

INTRODUCTION

Collimation with Hollow Electron Lenses (HELs) [1-2] gives a means of depleting the transverse tails of the circulating beam without using intercepting material, thereby avoiding the risk of damage and not contributing to machine impedance.

In order not to perturb the core of the circulating beam, the hollow electron beam shall have a negligible residual field at the centre of the electron column, and hence, must be circular and with uniform electron transverse distribution. Parameters that affect the electron beam dynamics, such as the electron current and current density, energy, the lens magnetic field, dimensions and geometrical configuration of vacuum chambers, therefore need to be carefully specified.

In this paper we aim to reproduce the experimental results measured at the Fermilab electron-lens test stand using simulations with CST Particle Studio. This allows us to study the influence of imperfections such as gun and magnet misalignment, and non-uniform current yield, which will be further studied at the CERN Electron Lens test stand, currently under construction. Understanding these parameters, and benchmarking the simulations is very important to predict the shape of high current electron beams.

ELECTRON BEAM DYNAMICS

The criteria of beam stability for hollow electron beams with a homogeneous current distribution in a uniform magnetic field were described by Davidson in [3], and the influence of the shape profile on the diocotron instability was studied in [4].

Let's consider an annular, low-density ($\omega_{pe}^2 \ll \omega_{ce}^2$), non-neutral electron plasma confined radially by a uniform, axial magnetic field B, where ω_{pe} and ω_{ce} are the electron plasma frequency and electron cyclotron plasma frequency respectively. The radial, self-electric field of the electron beam combined with the longitudinal confining magnetic field causes a rotation of the electron column with angular velocity $\Omega(r)$:

$$\Omega(r) = \Omega_D \left(1 - \frac{b^2}{r^2}\right) \tag{1}$$

$$\Omega_D = \frac{\omega_{pe}^2}{2\omega_{ce}} \tag{2}$$

where Ω_D is the diocotron frequency, b is the inner radius of the beam and r is the distance from the axis of the electron column, with r > b.

Assuming that the electrons emitted from the cathode have the characteristics of a non-relativistic Child-Langmuir flow, then, if V is the cathode-anode potential that determines the extracted current $I = \mu V^{3/2}$, where μ is the perveance, the maximum rotation phase φ of the electron column during its transit time ΔT can be expressed as

$$\varphi \approx \Omega_D \Delta T \approx \Omega_D \frac{L}{v_z} \approx const. \times \frac{\sqrt{V}}{B} L \tag{3}$$

where L is the length of the system and v_z is the axial velocity of the electron beam [5].

Furthermore, assuming that the evolution of the hollow electron beam profile depends on its rotation phase φ, we can predict the shape of the beam based on the scaling factor $\frac{\sqrt{V}}{B} L$.

EXPERIMENTAL MEASUREMENTS

E-lens Test Stand at FNAL

The Fermilab electron lens test stand [6-7] was built in the late 1990s to support the development of electron lenses for the Tevatron collider. Currently, it is being used to characterize the performance of electron guns and to study the dynamics of intense, magnetically confined electron beams. Recently, it has been used to test electron guns for the Fermilab Integrable Optics Test Accelerator (IOTA) [8] and to characterize high-current hollow electron gun prototypes for beam halo control in the High-Luminosity LHC [9-13]. The test stand includes a pulsed electron gun, a straight beamline, a collector and beam diagnostics equipment. The vacuum beam line is surrounded by three
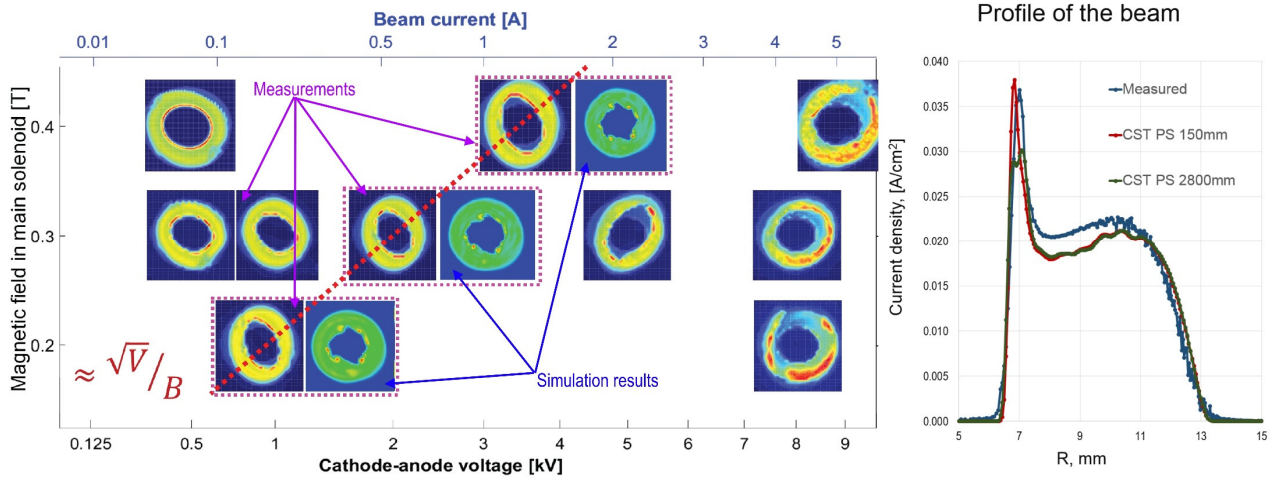
Figure 1: Measured and calculated profiles of the hollow beam depending on magnetic field in main solenoid and current of the beam (left), comparison of measured and simulated profiles (right).

solenoid magnets: gun solenoid, main solenoid and collector solenoid. The electron beam can be deflected by steering coils inside the main solenoid, allowing the beam to be swept through a fixed pin-hole FC at the collector to measure the transverse beam profile.

Experimental Measurements

Figure 1 shows measurements of the electron beam profile as a function of the magnetic field B_z in the main solenoid and the applied cathode to anode voltage difference at the electron gun. The cathode-anode voltage defines the extracted current.

The experimental measurements are in good agreement with theoretical predictions, with the same beam shape maintained for constant scaling factor ($\sqrt{V}/B$), as shown by the red dotted line in Fig. 1. High current beam in a low magnetic field is distorted much more than a low current beam in a high magnetic field. At constant magnetic field the total rotation phase is bigger at larger beam currents.

These measurements were performed with the hollow electron gun named CHG1b. This electron gun was a prototype built at CERN based upon a Fermilab design. These measurements can be used for benchmarking the computer simulation models and for commissioning the E-lens test stand currently under construction at CERN.

NUMERICAL SIMULATIONS RESULTS

Numerical simulations were performed in CST Particle Studio (CST PS). This is a specialized tool for the analysis and modelling of charged particle dynamics in 3D electromagnetic fields. The particle-tracking solver can model the behaviour of particles through electro-magnetic fields, and incorporates space charge limited emission [14].

Each simulation was split into to two sub-tasks: modelling of the gun emission and modelling the beam dynamics. Particles were transferred from one task to the other using the export/import interfaces of CST PS.

E-gun Simulations

The cross-section of gun CHG1b is shown in Fig. 2. The outer and inner diameters of the cathode (shown in red) are 25.4 mm and 13.5 mm respectively. The cathode emitting surface has a radius of curvature of 10 mm with a chamfer of 0.5 mm. The cathode is surrounded by a focusing electrode (yellow) and a control electrode (blue).

Simulations of the E-gun were performed using the space-charge model of electron emission in CST PS. To validate the simulation settings and parameters of the emission model a parametrical model of a spherical diode was initially simulated. Changing the radius of the inner electrode (emitter), the mesh size, and parameters of the emission model, the results were compared with the analytical solution derived by Langmuir and Blodgett [15]. The settings that gave the best agreement were used for the E-gun simulations.
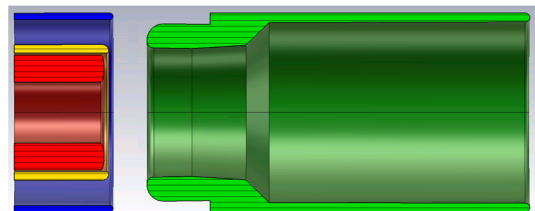
Figure 2: Cross-section of the CHG1b E-gun.

Calculations of perveance were performed, with the resulting perveance of $\mu = 6.6$ A/V$^{2/3}$ in good agreement to the $\mu = 6.5 \pm 0.1$ A/V$^{2/3}$ measured at the E-lens test stand at FNAL.

The comparison of the measured emission profile with simulations is shown in Fig. 1 (profile after 150 mm and 2800 mm from the cathode shown is read and green respec-tively). It should be noted that measurement of the beam profile was carried out after 2.8 m of drift. To minimize E×B distortions, configuration with low current electron beam (75 mA) in a high magnetic field (0.4 T) was chosen.

Electron Beam Dynamics

As a next step, measurements of beam dynamics were simulated. For comparison, the results of three simulations are shown in Fig. 1. The simulations exhibit a similar general behaviour of the beam when compared to the experimental results, but show less distortion.
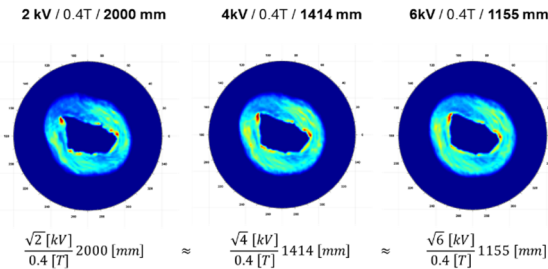
Figure 3: Examples of profiles with tilted injection.

Imperfections (gun and solenoids misalignments, non-uniform current yield, etc.) can significantly change the beam profile. Figure 3, for example, shows the transverse profile of the electron beam after 2.8 m obtained with a gun tilted by 2° with respect to the longitudinal axis. For comparison, in Fig. 4 (middle) transverse profile from the non-tilted gun with the same parameters (4 kV in 0.4 T) is shown. Again, in agreement with theoretical predictions, the distorted beam profiles look similar if the path length, voltage and magnetic field satisfy the constant scaling factor condition.

DATA ANALYSIS

One can clearly distinguish three regions in the beam profile shown in Fig. 1: an inner peak with high current density, a central plateau and an outer decay. Every layer of the hollow electron beam rotates with different angular velocity (Eq. 1). It is therefore desirable to have a technique that would allow a comparison of the amplitude and angular offset of each individual layer. This can be achieved by comparing their polar Fourier transforms.

Polar Fourier Transform

Since the beam profiles have rotational symmetry, it is convenient to use polar coordinates. Using a Fourier transform in polar coordinates, the function $f(r, \varphi)$ can be decomposed into a sum of basic functions $\Psi(k, m)$ with certain amplitudes [16]:

$$f(r, \varphi) = \sum_{k=1}^{\infty} \sum_{m=-\infty}^{\infty} P_{km} \Psi_{km}(r, \varphi) \qquad (4)$$

$$\Psi(k, m) = \sqrt{k} J_m(kr) \Phi_m(\varphi) \qquad (5)$$

where $\Phi_m(\varphi) = \frac{1}{\sqrt{2\pi}} e^{im\varphi}$ and J_m is the m-th order Bessel function.

Coefficients P_{km} are defined by:

$$P_{km} = \int_0^a \int_0^{2\pi} f(r, \varphi) \Psi_{km}^*(r, \varphi) r dr r d\varphi \qquad (6)$$

Results

The polar Fourier decomposition of the symmetrical and distorted beam profiles are shown on Fig. 4. A symmetric,

undistorted beam has only "zero" modes (P_{k0}), while a distorted beam has higher harmonics that define the shape, position and rotation phase of the areas of disturbance.
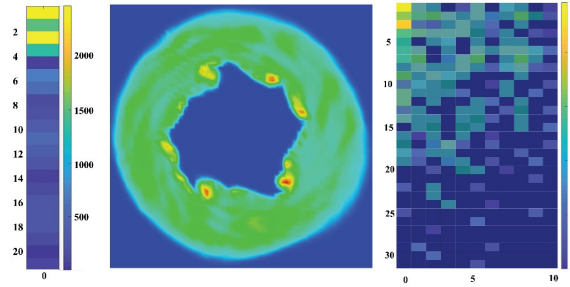
Figure 4: Polar Fourier decomposition of uniform and distorted beams: real part of coefficients P_{k0} for a uniform beam (left), the distorted beam image (middle), coefficients P_{km} for the distorted beam (right).

This technique will be used for data analysis during the commissioning E-lens test stand at CERN.

E-LENS TEST STAND AT CERN

An E-lens Test Stand is currently being constructed at CERN, composed of a pulsed electron gun with a straight beamline, surrounded by a gun solenoid and a collector solenoid. In between the two solenoids a diagnostic box with a Pin Hole Faraday Cup and a YAG:Ce screen will be installed. The collector will be a passively cooled annular Faraday Cup with repelling electrode to ensure all secondaries created do not escape. A viewport at the collector will allow visual inspection of the cathode and the uniformity of the current yield to be checked.

The E-lens Test Stand will be used for e-gun characterization, measuring the current emission yield as a function of cathode temperature and as a function of the extraction voltage, measuring the beam profile with varying magnetic field at the gun and anode-cathode voltage, and cross-checking the numerical models of computer codes.

CONCLUSIONS

Electron beam dynamic simulations of a hollow electron gun with different configurations of current and magnetic fields were performed in CST PS.

The estimated perveance and initial profile of the electron beam is in a good agreement with experimental results. The dynamics of the simulated beam follows theoretical predictions, however the profiles obtained in simulation are much less distorted when compared to experimental results. It was shown that both imperfections of the electron gun and the settings of the computer model affect the results and should be studied in more details. With the beam diagnostics only at the end of the drift solenoid, it is difficult to determine the reason for these discrepancies.

The CERN E-lens test stand will give additional capabilities for e-gun characterization, allowing measurements of the beam profile just after extraction from the gun, without drift. This will enable further optimisation of both the gun design and subsequent transport through the electron lens, through benchmarked simulation codes.

REFERENCES

[1] G. Stancari, A. Valishev, G. Annala, G. Kuznetsov, V. Shiltsev, D. A. Still, and L. G. Vorobiev, "Collimation with Hollow Electron Beams", *Phys. Rev. Lett.* 107, 084802 (2011).

[2] X. Zhang, V. Kamerdzhiev, A. L. Romanov, V. D. Shiltsev, and A. Valishev, "Tevatron Electron Lens and its Applications", in *Proc. 7th Workshop on Beam Cooling and Related Topics (COOL'09)*, Lanzhou, China, Aug.-Sep. 2009, paper THM1MCCO02, pp. 103-106.

[3] R. C. Davidson, *An Introduction to the Physics of Nonneutral Plasmas* (Addison-Wesley, 2001).

[4] R. C. Davidson and G. M. Felice, "Influence of profile shape on the diocotron instability in a non-neutral plasma column", *Phys. Plasmas* 5, 3497 (1998).

[5] Y. H. Jo, J. S. Kim, G. Stancari, M. Chung, and H. J. Lee, "Control of the diocotron instability of a hollow electron beam with periodic dipole magnets", *Physics of Plasmas* 25, 011607 (2018).

[6] The Fermilab electron-lens test stand, https://cdcvs.fnal.gov/redmine/projects/elens/wiki/Test_Stand

[7] C. Crawford *et al.*, "Prototype 'Electron Lens' Set-up for the Tevatron Beam-Beam Compensation," in *Proc. 18th Particle Accelerator Conf. (PAC'99)*, New York, NY, USA, Mar. 1999, paper TUCR5, pp. 237-239.

[8] S. Antipov *et al.*, "IOTA (Integrable Optics Test Accelerator): Facility and Experimental Beam Physics Program," JINST 12, T03002 (2017), http://dx.doi.org/10.1088/1748-0221/12/03/T03002

[9] G. Stancari *et al.*, Conceptual design of hollow electron lenses for beam halo control in the Large Hadron Collider, FERMILAB-TM-2572-APC, CERN-ACC-2014-0248, https://arxiv.org/abs/1405.2033

[10] G. Stancari, V. Previtali, A. Valishev, R. Bruce, S. Redaelli, A. Rossi, and B. S. Ferrando, Fermilab Report No. TM-2572-APC (2014); e-print arXiv:1405.2033 [physics.acc-ph].

[11] C. Zanoni, G. Gobbi, D. Perini, and G. Stancari, "Preliminary Mechanical Design Study of the Hollow Electron Lens for HL-LHC", in *Proc. 8th Int. Particle Accelerator Conf. (IPAC'17)*, Copenhagen, Denmark, May 2017, pp. 3547-3550. doi:10.18429/JACoW-IPAC2017-WEPVA117

[12] S. Li and G. Stancari, "Characterization of an Electron Gun for Hollow Electron Beam Collimation", FERMILAB-TM-2542-APC (August 2012).

[13] V. Moens, "Experimental and numerical studies on the proposed application of hollow electron beam collimation for the LHC at CERN", Master thesis, Ecole Polytechnique, Lausanne, Switzerland, 2013.

[14] H. Spachmann and U. Becker, "Electron gun simulation with CST PARTICLE STUDIO", *Nuclear Instruments and Methods in Physics Research,* A 558 (2006) 50–53.

[15] I. Langmuir and K. B. Blodgett, "Current limited by space charge between concentric spheres," *Phys. Rev.* 24, 49 (1924).

[16] Q. Wang, O. Ronneberger and H. Burkhardt, "Rotational Invariance Based on Fourier Analysis in Polar and Spherical Coordinates", *IEEE Transactions on Pattern Analysis and Machine Intelligence*, 9-31, pp. 1715-1722, 2009.

MC5: Beam Dynamics and EM Fields

D11 Code Developments and Simulation Techniques